Supplemental Information

Figure S1: Time montage showing a secondary actin bundle left behind by the protruding lamellipodium (yellow arrowhead). This bundle merges with the newly formed actin arc (red arrowhead) during edge retraction.

Figure S2: Focal adhesion slippage occurs during edge retraction. a) Schematic showing what time segmentation of focal adhesion movement quantified in b) and c). b) Total focal adhesion translocation during the protrusion phase of edge motion. c) Total focal adhesion translocation during the retraction phase of edge motion.

Figure S3: Actin arc coupling to nascent adhesions advances the edge's protrusion retraction cycle. a) Time montage of paxllin-mCherry and actin-mGFP over three protrusion retraction cycles. Yellow arrowheads denote nascent adhesions and white arrowheads denote actin arc retraction between nascent adhesions. b-c) Paxillin (green) and actin (red) kymographs from line 1 (b) and line 2 (c) in (A). Line 1 is adjacent to the nascent adhesion formation and line 2 is a region directly on the adhesion. The number of protrusion/retraction cycles are labeled in (b). Arrowheads denote nascent adhesion formation. (c) Yellow arrowhead denotes rearward movement of the nascent adhesion and blue arrowhead denotes maturation. Red arrowheads denote the advance of the location of the base of the protrusion/retraction cycle after adhesion maturation. d) Time-montage of the box in (a). White arrowheads denote the appearance, yellow arrowheads denote the rearward movement, and blue arrows denote the maturation of adhesion.

Figure S4: Oscillatory edge motion at the leading edge of migrating fish keratocyes. Fish keratocytes have long been a favored model for cell migration because of their extremely fast migration rates. Although, electron microscopy studies have shown keratocytes have prominent myosin II-laden actin arcs, it has been assumed that their edge only protrudes, and, thus, does not display oscillatory motion [1, 2]. We found that the published data was not sufficient to distinguish whether or not fish keratocytes had oscillatory edge motion. Therefore, we cultured keratocytes as previously described[3] from the scales of *Poecilia latipinna*. We then acquired differential interference contrast time-lapse recordings of single crawling cells with images acquired every second. a) shows one frame of a time-lapse DIC recording of one of these crawling cells (dotted line shows orientation of kymographs). b-c) Kymographs are presented for three cells that are moving quickly (b) and slowly (c) relative to each other. All cells analyzed show edge oscillations (arrowheads). These oscillations do not always, but indeed can, result from an edge retraction, but, instead, a slowing of the edge protrusion. Cell body and cell velocity are indicated in the kymograph for each cell. Actin arc formation has been shown to be cyclical and myosin II-dependent in the neuronal growth cone with little, if any edge oscillations. It is important to notes that these studies were done using growth cones on poly-D-lysine coated

coverslips on which growth cones do not extend. In contrast, neuronal growth cones plated on permissive growth substrates do show a robust edge oscillatory cycle identical to the motion presented here. The similarity in actin filament organization between the keratocyte[1], neuronal growth cone [4, 5], and PtK1 cells (Fig. 1) gives further support that these cells could use the same mechanism for motility.

Supplemental Movie Legends

Movie S1: Raw time-lapse recording of actin-tdEOS molecules at the leading edge. Epi-fluorescence. Images acquired every 5 seconds. Movie height: 33 mm. Movie length: 15.3 min.

Movie S2: Time-lapse recording of actin-RFP expressed in a PtK1 cell. Spinning disk confocal. Images acquired every 20 seconds. Movie height: 39 μm. Movie length: 60 min.

Movie S3: Time-lapse recording of actin-RFP (red) and myosin IIA-GFP (green) at the leading edge. Myosin IIA-GFP channel intensity was stretched to reveal the small amount of myosin in the lamellipodium. Spinning disk confocal. Images acquired every 10 seconds. Movie height: 31 μm. Movie length: 25.8 min.

Movie S4: Time-lapse recording of a mouse melanoma cell (B16-F1) expressing actin-mRFP. Note the cycle of actin arc assembly and disassembly underlying edge motion. It has been shown that actin filaments from the filopodial actin bundles (see prominent actin bundles a the leading edge) can be added to the actin arc bundles[6]. How this modification changes edge growth will be an interesting direction of future investigation. We focused our current study on actin arcs in cells that lack filopodial actin bundles for several reasons. First, actin arc assembly occurs in cells lacking filopodia[1]. Secondly, it has been shown that actin arc formation is unimpeded by filopodial actin bundle removal[4]. Taken together, this would indicate that the basal mechanism of actin arc format ion is independent of filopodia. B16-F1 cells were cultured as previously describe[6]. Images were acquired every 5 seconds. Movie height: 61 μm. Movie length: 14 min.

References for Supplemental Information

1. Svitkina, T. M., Verkhovsky, A. B., McQuade, K. M. & Borisy, G. G. Analysis of the actin-myosin II system in fish epidermal keratocytes: mechanism of cell body translocation. J Cell Biol 139, 397-415 (1997).
2. Machacek, M. & Danuser, G. Morphodynamic profiling of protrusion phenotypes. Biophys J 90, 1439-52 (2006).
3. Theriot, J. A. & Mitchison, T. J. Actin microfilament dynamics in locomoting cells. Nature 352, 126-31 (1991).
4. Burnette, D. T., Schaefer, A. W., Ji, L., Danuser, G. & Forscher, P. Filopodial actin bundles are not necessary for microtubule advance into the peripheral domain of Aplysia neuronal growth cones. Nat Cell Biol 9, 1360-9 (2007).
5. Mongiu, A. K., Weitzke, E. L., Chaga, O. Y. & Borisy, G. G. Kinetic-structural analysis of neuronal growth cone veil motility. J Cell Sci 120, 1113-25 (2007).
6. Nemethova, M., Auinger, S. & Small, J. V. Building the actin cytoskeleton: filopodia contribute to the construction of contractile bundles in the lamella. J Cell Biol 180, 1233-44 (2008).

Figure S1- Lippincott-Schwartz

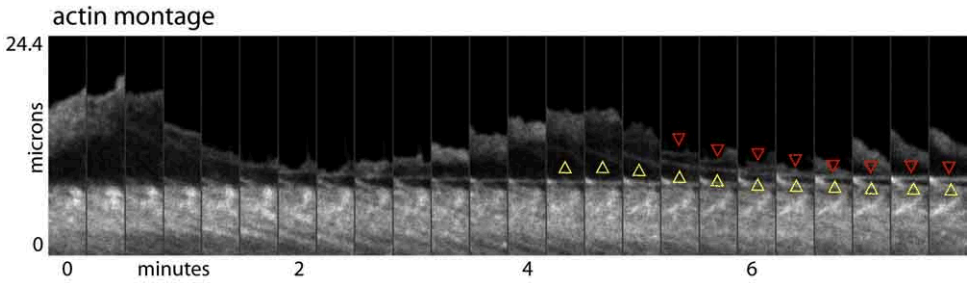

Figure S2- Lippincott-Schwartz

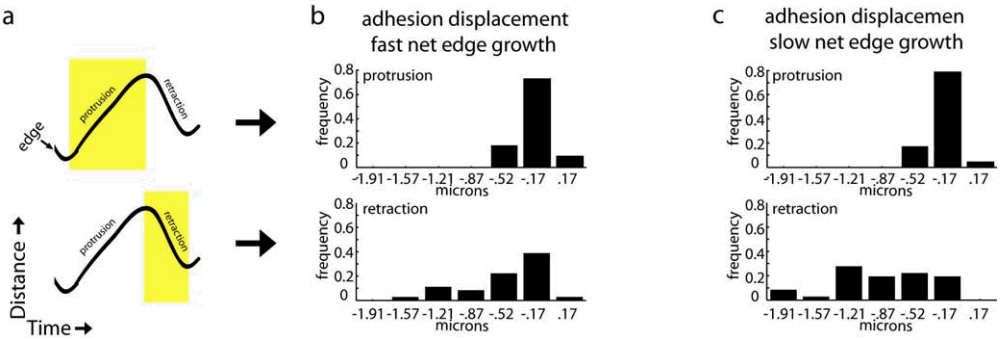

Figure S3- Lippincott-Schwartz

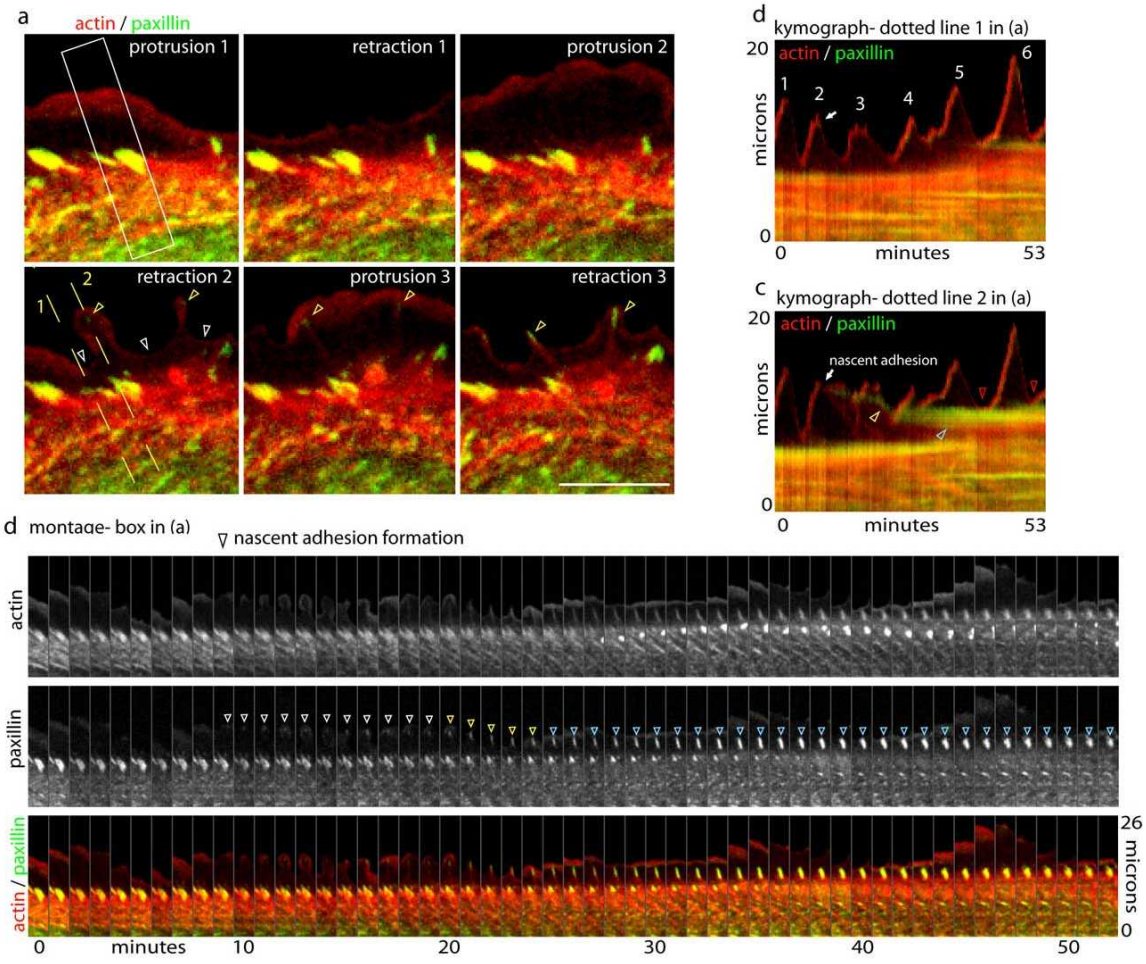

Figure S4- Lippincott-Schwartz